Contents lists available at ScienceDirect

Electrochimica Acta

journal homepage: www.elsevier.com

Combined effect of alkaline cations and organic additives for iodide ion conducting gel polymer electrolytes to enhance efficiency in dye sensitized solar cells

T.M.W.J. Bandara[a, b], H.D.N.S. Fernando[a, b], M. Furlani[c, *], I. Albinsson[c], J.L. Ratnasekera[b], L. Ajith DeSilva[d], M.A.K.L. Dissanayake[e], B.-E. Mellander[a]

[a] *Department of Physics, Chalmers University of Technology, Gothenburg, Sweden*
[b] *Department of Physical Sciences, Rajarata University of Sri Lanka, Mihintale, Sri Lanka*
[c] *Department of Physics, University of Gothenburg, Gothenburg, Sweden*
[d] *Department of Physics, University of West Georgia, Carrollton, GA 30118,USA*
[e] *National Institute of Fundamental Studies, Kandy, Sri Lanka*

ARTICLE INFO

Article history:
Received 23 January 2017
Received in revised form 6 August 2017
Accepted 7 August 2017
Available online xxx

ABSTRACT

Iodide ion conducting electrolytes are intensively studied as effectual electrolytes for dye-sensitized solar cells (DSSCs). However, the nature and concentration of the counter-ion (cation) in the electrolyte exert a profound influence on the performance of the thin film meso-porous TiO_2 based DSSCs. A series of gel electrolytes containing the alkaline iodides LiI, NaI, KI, RbI and CsI and polyacrylonitrile (PAN) were fabricated together with the non-volatile plasticizers ethylene carbonate (EC) and propylene carbonate (PC). A similar series was fabricated with the inclusions of performance enhancers (additives) tetrapropylammonium iodide (Pr_4NI), the ionic liquid 1-methyl-3-propyl imidazolium iodide (MPII) and 4-tert-butylpyridine (4TBP). The ionic conductivity of the electrolytes was studied in order to investigate its dependence on the nature of the alkaline cation in presence or absence of additives. The conductivities were higher for the electrolytes with the larger cations, namely K^+, Rb^+ and Cs^+. A significant conductivity enhancement was observed in presence of the additives, and this effect was especially noticeable for samples with the smaller cations. The highest conductivity for electrolytes with additives, 3.96 mS cm^{-1} at 25 °C, is exhibited by KI containing samples.

© 2017.

Quasi-solid state DSSCs were assembled using the above mentioned series of gel electrolytes and TiO_2 photo-anodes prepared with a meso-porous TiO_2 layer overlaid on a compact spin coated layer of the same oxide. A clear trend of open circuit voltage (V_{oc}) and efficiency enhancement with increasing cation size is observed for additive free cells. However, additives enhanced the V_{oc}, short circuit current density (J_{sc}), fill factor (*ff*) and energy conversion efficiency in all the series of DSSCs investigated. All the cells with additives have shown V_{oc} and *ff* higher than 0.7 V and 60% respectively. The maximum J_{sc} and efficiency were given by KI based DSSC reaching 11.35 mA cm^{-2} and 5.26%. The performance enhancers or additives used in this work are responsible for 348.0, 216.9, 76.5, 35.8 and 22.4% efficiency enhancement for LiI, NaI, KI, RbI and CsI containing solar cells, respectively.

1. Introduction

Dye sensitized solar cells are getting progressively more interest since studies show the feasible actuation with the use of gel polymer electrolytes [1–3]. This approach to the construction of the cells has the main advantage to reduce the desorption process of the dye from the photoanode operated by the pure organic solvents. In fact, solvents like organic carbonates, that as pure solvents could contribute to the desorption of the dye, may instead interact with the polymeric gelling agent, for example polyacrylonitrile when they are confined. In this way they play a less strong role in the interaction with the dyes. The rather different properties of a solvent confined in a gel structure are generally observed, as for example in the field of art conservation [4]. Therefore, the use of polymer gel electrolytes results in more durable devices. Other practical advantages are the low volatility, the easier lamination and confinement by a simple thermo-sealant during the fabrication [5]. Although DSSCs based on liquid electrolytes are reported to have better efficiencies [6–8], development of quasi-solid-state or all solid state solar cells is highly important in order to fabricate commercially viable DSSCs [1–3].

The selection of polymer gel electrolytes with high ionic conductivity, good compatibility with the photoanode, the ability to realize a high enough difference of potential at the TiO_2/electrolyte interface and to reduce the recombination phenomena is essential for the development of these materials [3,9,10]. The most commonly used redox couple is I^-/I_3^- making of the iodides a viable category of salts, but the cation and the salt concentration have a relevant role to play both in coordinating and stiffening the system influencing the mobility of the iodide and tri-iodide anions. The role of some organic additives has previously been investigated by us in order to optimize power

* Corresponding author.
Email address: f6bmauri@chalmers.se (M. Furlani)

https://doi.org/10.1016/j.electacta.2017.08.041
0013-4686/© 2017.

UNCORRECTED PROOF

output for LiI and RbI based systems [11], the cation concentration influence has been examined in a different work [12] and the role of the cation size in earlier work [13,14].

In the recent past quasi-solid state DSSCs have gained a significant development and some important findings have been reported. For instance Ardad et al. [15] have demonstrated an efficiency of about 8.90% by using a carbon counter electrode and PEO and PVDF-HFP based gel electrolyte. High electro-catalytic activity at the counter electrode/electrolyte interface and low charge transfer resistance are responsible for the higher solar cell performances. The cost reduction of the counter electrode and the reported higher efficiency are important observations [15]. In addition, Andrade et al. [16] have prepared quasi-solid-state DSSCs using organo-talcs as a gelator and they reported efficiencies higher than in the respective liquid counterparts. The degradation of cell performances has been reduced by intercalating poly-iodides into the inter-lamellar space of the talc. The quasi-solid solar cell containing the poly-iodides have maintained 95% of their initial efficiency under light-soaking at 1 Sun for about 1000 h. The quasi-solid solar cell has shown an efficiency above 95% of their initial value under light-soaking at 1 Sun for about 1000 h. The flexible quasi-solid DSSC based on plastic substrates and metallic meshes reported by Gerosa et al. is also an important step towards preparing portable cells [17]. Several methods of investigation have been developed to characterize the electrolyte in the devices with optical and electrochemical techniques. Among these electrochemical impedance spectroscopy and potentio/galvanostatic measurements have given important results [18].

In this work a series of gel electrolytes containing alkaline iodides LiI, NaI, KI, RbI and CsI and polyacrylonitrile (PAN) together with the non-volatile plasticizers ethylene carbonate (EC) and propylene carbonate (PC) were fabricated. Selected additives which do not degrade the physical and chemical stability of the electrolyte and DSSC were incorporated into the electrolyte with the intention of improving the energy conversion efficiency in solar cells [19,20]. Pr_4NI, MPII and 4TBP were selected to be incorporated as additives in the electrolyte series based on alkaline iodide salts. The conductivity behavior in the electrolyte and the influence on the solar cell performance were also investigated by means of EIS, infrared spectroscopy and potentiostatic methods.

2. Experimental

2.1. Materials

Alkaline metal iodides MI (M = Li, Na, K, Rb, Cs), polyacrylonitrile (PAN, MW = 150000), iodine (I_2), ethylene carbonate (EC) and propylene carbonate (PC) with purity greater than 98% were purchased from Aldrich. Prior to use, PAN was vacuum dried for 6 h at 50 °C and the alkaline metal salts for 6 h at 100 °C, both in a vacuum oven (10^{-3} mbar). The other materials were used as received. Conducting glass containing fluorine doped tin oxide (FTO) with a sheet resistance of 15 Ω cm^{-2} and sensitizing dye N719 were purchased from Solaronix SA. TiO_2 of two different particles sizes, P25 and P90, were received from Degussa.

2.2. Electrolyte sample preparation

Five different gel electrolyte samples were prepared according to the stoichiometric formula $(AN)_{10}(EC)_{25}(PC)_{20}(MI)_{1.2}(I_2)_{0.12}$ in order to keep the molar concentration of the electrolyte constant. In this formula AN represents one repeating unit of polyacrylonitrile and MI = LiI, NaI, KI, RbI or CsI. For electrolyte preparation, weights of PAN (0.1 g), EC (0.4151 g) and PC (0.3851 g) were kept unchanged. The compositions and the other ingredients in the electrolytes are given in Table 1. Initially, the appropriate amounts of EC, PC and salts were mixed in a closed glass bottle by continuous stirring at room temperature; when the salt was solubilized, PAN was added to the mixture, which was stirred at 100 °C for further 10 min to obtain the consistency of a gel. Finally, iodine was added to the mixture at 100 °C and let the electrolyte cool down to room temperature while the stirring was continued for a few more minutes. This procedure yielded a brown and homogeneous gel-type polymer electrolyte.

Another set of electrolytes was prepared using similar procedure but incorporating as additives tetrapropylammoniumiodide (Pr_4NI), 1-methyl-3-propyl imidazolium iodide, ionic liquid (MPII) and 4-tert-butylpyridine (4TBP). Weights of the additives in the electrolyte are given in Table 2.

2.3. Fabrication of DSSCs

Two layers of TiO_2 were deposited on the conducting glass substrate in order to prepare the photo-anode. The first layer or compact layer was spin-coated on a pre-cleaned FTO substrate using a colloidal suspension of TiO_2 P90 powder. The second layer (porous layer) was coated on the first layer using a colloidal suspension of TiO_2 P25 powder using the doctor blade method. The TiO_2 photo-anode preparation has been described in detail in a previous work [21]. The dye adsorption to the double layered TiO_2 film prepared on a FTO substrate was conducted by immersing the TiO_2-coated FTO plates in a 0.5 mM ethanolic solution of N719 dye for about 24 h at room temperature. Finally, the dye-adsorbed TiO_2 electrode was rinsed with acetone to remove the unbound TiO_2 particles and dye prior to assembly of the cells.

The prepared gel electrolyte was casted onto the dye-sensitized TiO_2 electrode and then a platinum (Pt)-coated conducting glass plate (counter electrode) was pressed on the top of the TiO_2 electrode to assemble a DSSC with the configuration glass/FTO/TiO_2/dye/electrolyte/Pt/glass.

2.4. Electrochemical Impedance Spectroscopy measurements

The impedance measurements were made on gel electrolyte samples with a thickness of ~ 0.2 mm sandwiched between two stainless (SS) steel electrodes of ~ 7 mm, using a computer-controlled

Table 1
Composition of electrolyte $(AN)_{10}(EC)_{25}(PC)_{20}(MI)_{1.2}(I_2)_{0.12}$ series. The weight of PAN (0.1 g), EC (0.4151 g) and PC (0.3851 g) were kept fixed.

Sample name	(MI)Salt/mg	I_2/mg
LiI	30.384	5.76
NaI	34.025	5.76
KI	37.682	5.76
RbI	48.208	5.76
CsI	58.977	5.76

Table 2
Composition of the electrolyte series containing additives (chemical composition $(AN)_{10}(EC)_{25}(PC)_{20}(MI)_{1.2}(Pr_4NI)_{0.75}(MPII)_{0.25}$ $(4TBP)_{0.85}$ $(I_2)_{0.12}$). The weight of PAN (0.1 g), EC (0.4151 g) and PC (0.3851 g) were kept fixed.

Sample Name	Salt (MI)	(MI)Salt/mg	Pr_4NI/mg	MPII/mg	4TBP/mg
LiI-ad	LiI	30.384	44.3	12.6	21.7
NaI- ad	NaI	34.025	44.3	12.6	21.7
KI- ad	KI	37.682	44.3	12.6	21.7
RbI- ad	RbI	48.208	44.3	12.6	21.7
CsI- ad	CsI	58.977	44.3	12.6	21.7

UNCORRECTED PROOF

HP4274 impedance analyzer in the frequency range of 10 Hz-0.1 MHz. Prior to measurements the samples were heated to 60 °C and thereafter the temperature of the sample was varied from 60 to 0 °C, taking measurements at 10 °C intervals during the cooling runs. During the impedance measurements the SS/electrolyte/SS cells were kept inside a Faraday cage and the temperature was controlled using a water bath connected to a GRANT heating system (type KD, England) and a cooling system (HETOFRIGE, Denmark). A K type thermocouple connected to a HEWLETT PACKARD 344401A multimeter was used to measure the sample temperature.

2.5. Current voltage characteristics

Fabricated solar cells were illuminated using a LOT-Oriel class AAB, 1.5G, solar simulator with a 1000 W m^{-2} (one sun) irradiation in order to obtain current density versus cell potential (*J–V*) characteristics using a computer controlled eDAQ Potentiostat and e-coder. The position of the cells in the illuminated area was kept constant. The area of the cell exposed to light was 11 mm^2 and the scan rate was 100 mV s^{-1}

2.6. Infrared spectroscopy

Attenuated total reflectance (ATR) spectra were obtained at room temperature on a computer interfaced Bruker Alpha FTIR spectrophotometer equipped with a Platinum-ATR with a Ge crystal module, with a resolution of 1 cm^{-1}.

2.7. Transient current

Transient current measurements (DC polarization) were carried out at room temperature by sandwiching an electrolyte sample between two iodine non-blocking electrodes with the configuration of (stainless steel)/I_2/electrolyte/I_2/(stainless steel).

3. Results and discussion

The ionic conductivity of all samples was calculated from the complex dielectric measurement (Nyquist plots) using the intercept with the real axis. Fig. 1 shows variation of conductivity against inverse temperature (1000/T) for the electrolyte series $(AN)_{10}(EC)_{25}(PC)_{20}(MI)_{1.2}(I_2)_{0.12}$ without additives and in all cases they seems to follow a "Vogel Tammann Fulcher" (VTF) behavior [22,23]. The observed conductivity increase with temperature for all the electrolytes can be attributed to thermal activation of mobility and carrier density [24]. The electrolyte containing the smallest cation, Li^+, shows the lowest conductivities for all measured temperatures. The electrolytes containing K^+, Rb^+, and Cs^+ show similar temperature dependence for the conductivity. These three electrolytes exhibited the highest conductivity.

Fig. 2 shows variation of conductivity against inverse temperature (1000/T) for the electrolyte series $(AN)_{10}(EC)_{25}(PC)_{20}(MI)_{1.2}(I_2)_{0.12}$ with the additives Pr_4NI, MPII and 4TBP. The electrolytes with additives have shown significant conductivity enchantments compared to those without additives. This behavior can be attributed to an increase of the carrier density due to the addition of Pr_4NI and MPII. The additives Pr_4NI and MPII are iodine salts that carry large cations, in particular, MPII is an ionic liquid. When they are incorporated into the electrolyte, both salts increase the number of ionic species in the electrolytes, since they can dissociate to tetrapropylammonium, 1-methyl-3-propyl imidazolium and iodide ions. The dissociation is facilitated by solvents EC and PC in the electrolyte. In particular, both the iodides (additives) can increase the density of iodide ions in the electrolyte. On the other hand, the conductivity depends on the number of charge carriers and their mobility. Therefore, the increase of the density of charge carriers affected by the incorporated additives will, in turn, improve the conductivity.

As liquid additives, the ionic liquids could provide plasticizing effect to the electrolyte as reported by many authors [25–27]. MPII can impose a plasticizing effect to the electrolyte contributing to an enhancement of the mobility of the charge carriers by increasing polymer chain flexibility [24–26].

Fig. 3 shows the variation of conductivity with the type of iodide salt for the $(AN)_{10}(EC)_{25}(PC)_{20}(MI)_{1.2}(I_2)_{0.12}$ electrolyte series at different temperatures. The conductivity variation is in agreement with the earlier reported values [13]. The conductivity of electrolytes depends on mobility of ions, dissociation of salt, polymer crosslinking, ion coordination and shielding by polymer chains etc. As already discussed [13] these effects are linked to the charge density and the size of ions in the electrolyte. Due to the smaller size and higher charge density Li^+ can crosslink the polymer chains strongly reducing the

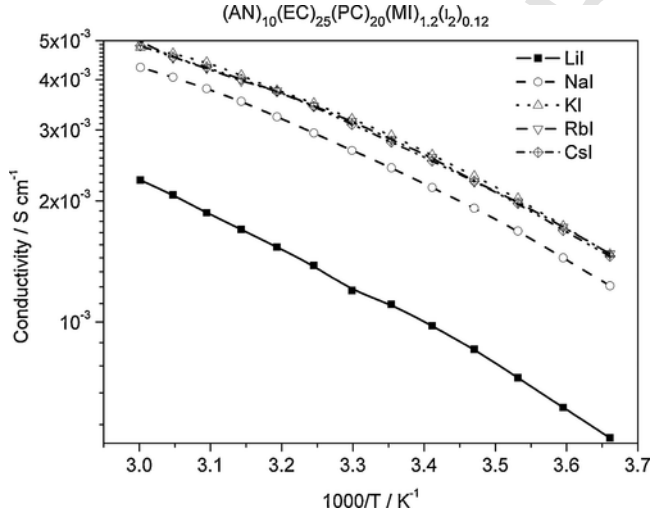

Fig. 1. variation of conductivity against inverse temperature (1000/T) in the electrolyte $(AN)_{10}(EC)_{25}(PC)_{20}(MI)_{1.2}(I_2)_{0.12}$ series without additives for different alkaline iodides.

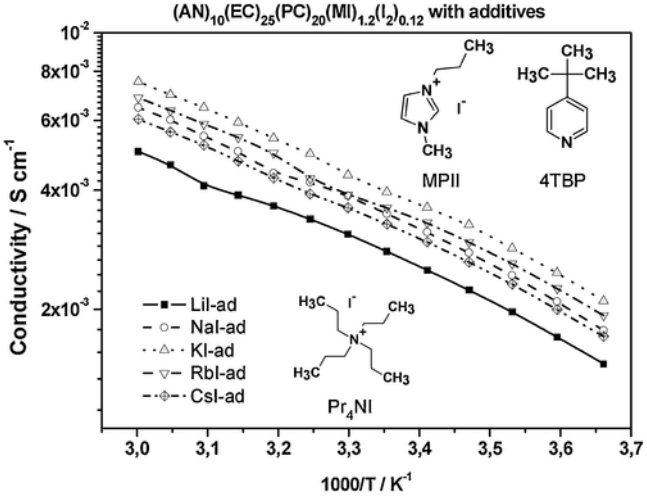

Fig. 2. variation of conductivity against inverse temperature (1000/T) in the electrolyte $(AN)_{10}(EC)_{25}(PC)_{20}(MI)_{1.2}(I_2)_{0.12}$ series with additives Pr_4NI, MPII and 4TBP (molecular formulas as insets) for different alkaline iodides.

PROOF

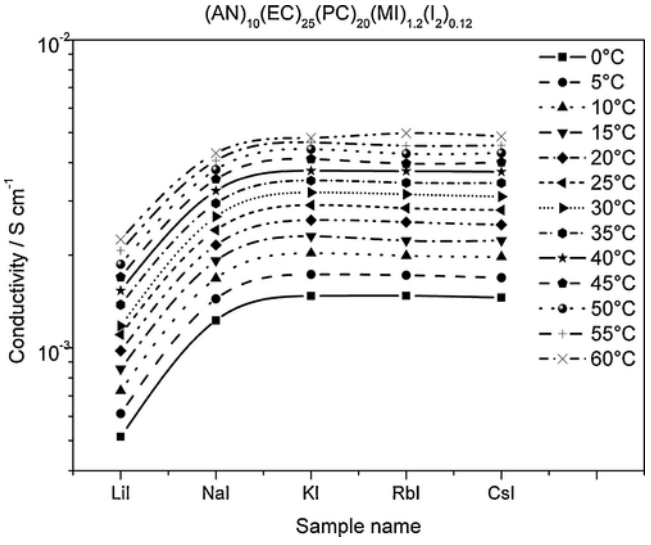

Fig. 3. Conductivity isotherms of the $(AN)_{10}(EC)_{25}(PC)_{20}(MI)_{1.2}(I_2)_{0.12}$ electrolyte series without additives.

polymer flexibility. This can result in reduction of mobility and density of free ions and thus the lowest conductivity is given by LiI containing electrolyte.

As seen in Fig. 3, all the electrolytes without additives have shown a similar trend for the conductivity variation and the curves have shifted upward with increasing temperature. These conductivity isotherms (Fig. 3) are clearly flattened in all cases and all temperatures for larger cations (K^+, Rb^+ and Cs^+) while in presence of additives (Fig. 4) there is a maximum for the KI and a minimum value for LiI.

The trend can be understood to some extent by studying diffusion coefficients and mobility of the alkaline ions since the molar composition of electrolyte was unchanged. Because, salts with larger cations (KI, RbI, and CsI) can be assumed to be completely dissociated and thus the concentration of ions in these electrolytes are unchanged. Therefore, the conductivity is governed by variation of mobility. Considering the availability of mobility data for the alkaline series of cations, the conductivity results obtained in our study are compared with results of liquid electrolytes. Mobility and diffusion coefficients of Li^+,Na^+, K^+,Rb^+,and Cs^+ at infinite dilution in water at 25 °C calculated from velocity autocorrelation functions are given in Fig. 4 [28]. Mobility and diffusion coefficients of K^+, Rb^+, and Cs^+ reach an almost common value compared to that of Li^+, Na^+ (Fig. 4). Therefore, flattening of conductivity in KI, RbI, CsI based gel electrolytes seen in Fig. 3 can also be correlated to unchanged mobility of the cations. However, the very low conductivity measured for the LiI electrolyte can be due to the cross-linking of the polymer chains by high charge density Li cations as mentioned above and by the large volume of the cation solvation shell.

Fourier transform infrared (FTIR) spectra of the samples were studied in order to understand the conductivity behavior by means of salt-gel interactions. The infrared spectroscopy offers little evidence of the stiffening action due to salts because the splitting or shifting of the gel characteristic peaks are hardly observable due to the relatively low dissociation of the iodides and because of the strong interaction of ethylene carbonate with the other gel components. The position of the CN stretching band is mainly tuned by the most polar EC [29]. We could anyway detect the typical splitting of the EC ring breathing mode at 893 cm^{-1} that for the sample containing LiI has a component around 900 cm^{-1} (Fig. 5) [30]. This effect was hardly visible for the sample with Na or other alkaline salts.

As previously observed using Raman spectroscopy on the same vibration [29], larger cations give even less splitting and at these concentrations not enough intense absorption. The absence of the split peak for the sample containing Li-I and additives can be explained by the competitive effect of the additives towards the Li cation, especially the nucleofilic 4TBP which results in a less intense coordination of the alkaline ion with EC and indirectly with the polymer backbone. The modest dilution effect due to the additives would not alone explain the decreased if not diminished intensity of the splitting at about 900 cm^{-1} for the Li^+ containing sample. A tentative curve fitting of the ring breathing peak (region 875–915 cm^{-1}) is shown in Fig. 6 for the Li and Na containing samples, in absence of additives. Sample with other salts does not show signs of peak splitting. The introduction of Li or Na shows a deformation of the region interpreted as previously discussed and is more clearly visible in other more dissociated systems as a weak split peak at 900 cm^{-1}, respectively. The fitting in the Li containing sample indicate a moderate dissociation of

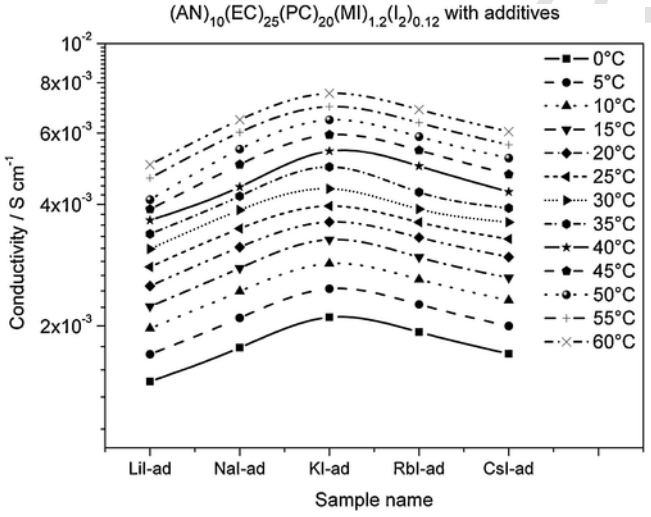

Fig. 4. Conductivity isotherms of the $(AN)_{10}(EC)_{25}(PC)_{20}(MI)_{1.2}(I_2)_{0.12}$ series with additives Pr4NI, MPII and 4TBP.

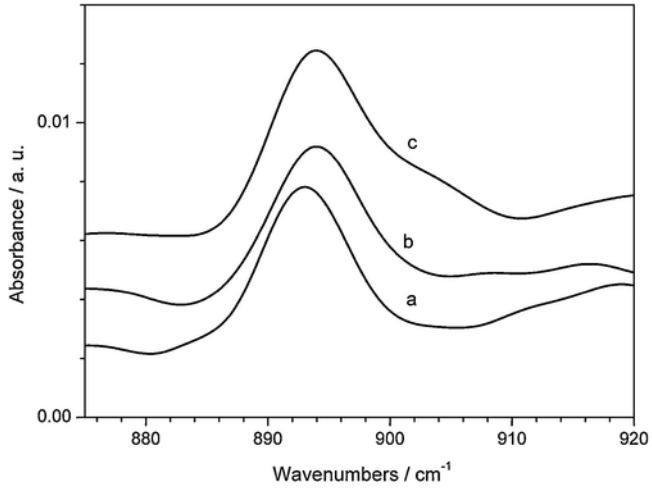

Fig. 5. ATR FTIR of the ring-breathing peak at 895 for EC a) PAN + EC + PC + additives b) PAN + EC + PC + LiI + additives c) PAN + EC + PC + LiI.

CORRECTED PROOF

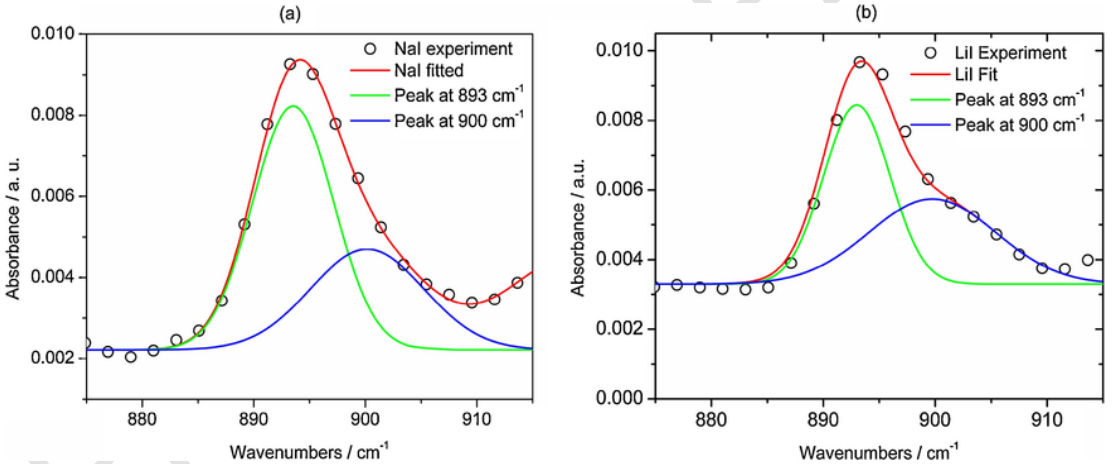

Fig. 6. Curve fitting of the gel containing (a) NaI and (b) LiI. a) Peak position 893 and 900 cm^{-1}, width 7.2 and 10 cm^{-1}, area 0.05 and 0.03 (a.u.); b) Peak position 893 and 900 cm^{-1}, width 5.4 and 11 cm^{-1}, area 0.03 and 0.04 (a.u.).

UNCORRECTED PROOF

the salt (for higly dissociated Li salts the intensity of the spilt peak can reach the same intensity as the original one). For the Na containing sample containing sample, where the salt is expected to be more dissociated, only a deformation of the peak is noticed and the fitting results were insufficient for an univocal evaluation and interpretation.

To explain the behavior of gels containing the larger alkaline cations we could consider that, in spite of larger coordination numbers, larger cations are less prone to form Lewis acid/base interactions due to their lower charge density in a model that can consider them of spherical symmetry. The larger coordination number is therefore not synonymous of strong bonds, but the increased bulkiness of the solvated cation can hinder a further increase of mobility because of the additives.

Fig. 7 shows the current density (J) versus cell potential (V) of the DSSCs containing the $(AN)_{10}(EC)_{25}(PC)_{20}(MI)_{1.2}(I_2)_{0.12}$ electrolyte series in absence of performance enhancers. The solar cell parameters short circuit current density (J_{sc}), open circuit voltage (V_{oc}), fill factor (*ff*) and energy conversion efficiency were calculated using the *J-V* curves shown in Fig. 7. Calculated parameters are given in Table 3. Very clearly the V_{oc} increases with the size of the cation in the electrolyte. The observed enhancement in V_{oc} with increasing size of the cation is now an established phenomenon [31] which can be attributed to the decrease of the recombination of electrons in the conduction band of TiO_2 with I_3^- in the electrolyte at the vicinity of the TiO_2 electrode and to the relative shift of the conduction band edge resulted by cation adsorption [13].

As shown in Table 3, the J_{sc} values of solar cells without additives increase with the cation size except for the one containing CsI. In general, the cation dependence of J_{sc} in a DSSC can be attributed to the variation of the iodide/triiodide conductivity and to the variation of charge injection rate from the dye to the TiO_2 influenced by the adsorbed cations [32].

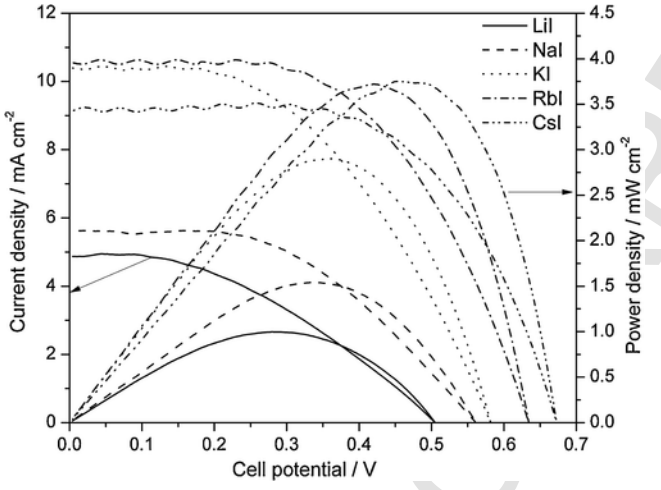

Fig. 7. Current density verses cell potential for the series of DSSCs containing the $(AN)_{10}(EC)_{25}(PC)_{20}(MI)_{1.2}(I_2)_{0.12}$ series without additives.

Table 3
solar cell parameter of the DSSC fabricated with alkaline iodides without additives.

Sample	t_-	V_{oc}/V	J_{sc}/mA cm^{-2}	*ff*/%	Efficiency/%
LiI	0.97	0.506	4.87	40.42	1.00
NaI	0.90	0.560	5.39	49.20	1.54
KI	0.79	0.582	10.40	49.23	2.98
RbI	0.76	0.636	**10.56**	55.39	3.72
CsI	0.67	**0.672**	9.14	**60.97**	**3.75**

Though the conductivity in KI, RbI, CsI electrolytes are similar, the performances of the respective solar cells are different. This trend can be understood since the conductivity of electrolyte is not the only factor governing the solar cell performance and the short circuit photocurrent (J_{sc}) in these DSSCs is mainly governed by the iodide/tri-iodide ion conductivity. The iodide and triode ion conductivity has profound influence on photocurrent density in a DSSC, since charge transport between photo-anode and Pt counter electrode is carried by iodide/tri-iodide redox couple [31]. In addition to iodide/tri-iodide conductivity the charge transfer rate at the two interfaces, particularly at the TiO_2/electrolyte also has a major influence on photo current density as the electron transfer dynamics of photogenerated electrons are governed by the shifted position of the TiO_2 conduction band edge due to cation adsorption by TiO_2 [30–32] Further, recombination kinetics also control the photocurrent.

As explained above, the J_{sc} variation cannot be due only to the net ionic conductivity. The transference numbers of the ions in the electrolytes are estimated using transient current measurement. For this purpose, electrolytes were sandwiched between two iodine (non-blocking) electrodes [33]. The estimated iodide ion transference numbers (t_-) of the electrolyte series are given in Table 3. Though net ionic conductivities of gel polymer electrolytes containing KI, RbI, CsI are similar their I^- ion transference numbers are different. The poor I^- ion conductivity, resulted by low transference number, has led to low photocurrent for CsI containing electrolyte compared to KI and RbI electrolytes. Conversely, DSSCs containing CsI exhibits highest efficiency due to superior V_{oc} resulted by upward shift of the conduction band due to the presence of larger cations. The higher I^- ion conductivity in RbI electrolyte resulted by the larger transference number compared to CsI based cell has led to the highest J_{sc} for the RbI based DSSC. J_{sc} in the DSSC containing KI reached a value closer to that of the RbI based cell due to higher I^- ion transference number. However, cell performances are relatively poor due to the drop of V_{oc} caused by the relatively small size of K^+ compared to Rb^+, and Cs^+.

The fill factor and the efficiency also increase with the size of the cation in the electrolyte as seen from Table 3. Therefore, it can be concluded that within the studied system the highest solar cell performances are offered by gel polymer electrolytes containing larger cations for samples exclusive of enhancers.

Fig. 8 shows the current density versus cell potential for the series of DSSCs containing the $(AN)_{10}(EC)_{25}(PC)_{20}(MI)_{1.2}(I_2)_{0.12}$ series inclusive of additives Pr_4NI, MPII and 4TBP. All the solar cells with additives have shown enhancement of all the cell parameters namely J_{sc}, V_{oc}, *ff,* and efficiency compared to that of cells without additives. As discussed above the ionic conductivity of in the electrolyte improves with added Pr_4NI and MPII. Therefore the J_{sc} enhancement with the two added iodides is an expected behavior. In addition, ionic liquid is known to give rise to micellar structures and different cation/anion stacking arrangements by influencing interfacial charge transport [34,35]. 4TBP is well known to improve the V_{oc} in DSSCS [36]. 4TBP could capture cations producing an increase of the dissociation of the iodides thus contributing to improve iodide ion conductivity.

Considering ionic conductivities given in Fig. 4 and J_{sc} values given in Table 4 it can be concluded that J_{sc} was governed by the ionic conductivity in the electrolyte as expected. According to data in Table 4, the variation of the energy conversion efficiency is governed by J_{sc}. Efficiency enhancement compared to that of additive free samples is given in Table 4 in order to estimate the effect for the efficiency due to additives Pr_4NI, MPII and 4TBP. When the size of the cation increases the effect of additives become less significant. Very significant efficiency enhancements were given for the DSSCs with

UNCORRECTED PROOF

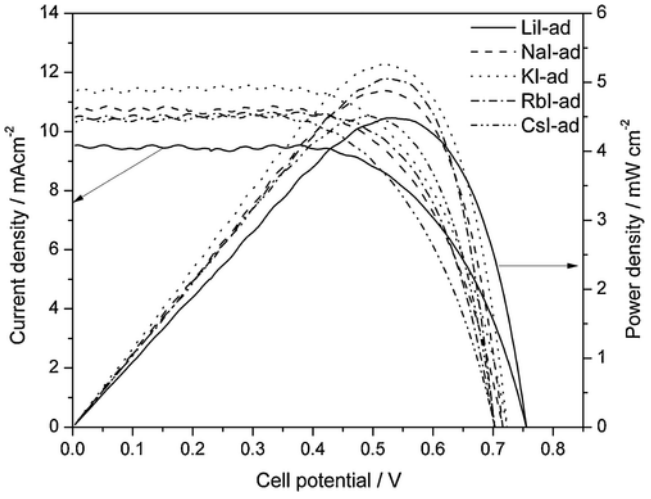

Fig. 8. Current density versus cell potential for the series of DSSCs containing the $(AN)_{10}(EC)_{25}(PC)_{20}(MI)_{1.2}(I_2)_{0.12}$ series with additives.

Table 4
Solar cell parameter of the DSSCs fabricated with alkaline iodides with additives, Pr_4NI, MPII and 4TBP and the efficiency enhancement due to additives.

Sample	V_{oc}/V	J_{sc}/mA cm^{-2}	*ff*/%	Efficiency/%	Efficiency Enhancement/%
LiI-ad	**0.756**	9.53	62.22	4.48	348.0
NaI- ad	0.718	10.77	63.11	4.88	216.9
KI- ad	0.724	**11.35**	63.99	**5.26**	76.5
RbI- ad	0.704	10.49	**68.45**	5.05	35.8
CsI- ad	0.702	10.33	63.30	4.59	22.4

electrolytes containing LiI and NaI. Additives have increased the efficiency by 348 and 217% in DSSCs based on LiI and KI, respectively.

Open circuit voltage and fill factor also increased with incorporated additives. All the cells with additives have shown V_{oc} and *ff* higher than 0.7 V and 60%, respectively. The maximum J_{sc} and efficiency are given by KI containing DSSCs, reaching 11.35 mA cm^{-2} and 5.26%, respectively. RbI containing cells also showed a 5.05% energy conversion efficiency. The reported work is important to make decisions on appropriate candidate salt to fabricate efficient DSSCs inclusive or exclusive of performance enhancers. A further analysis of the performance of the device through the study of light modulated EIS might face the possible variation of capacitance at the mesoporous layer for the different electrolytes composition but in this study the given explanation is based on the infrared and EIS analysis of the bulk properties of the electrolytes [37].

4. Conclusions

A series of electrolytes are prepared for DSSCs using the molar composition, $(AN)_{10}(EC)_{25}(PC)_{20}(MI)_{1.2}(I_2)_{0.12}$. The conductivity in the electrolyte series was improved by incorporating Pr_4NI, MPII and 4TBP as additives. For additive free samples the lowest conductivity is given by the LiI containing sample. The electrolytes containing K^+, Rb^+, and Cs^+ showed almost the same conductivity values and variation with temperature. The trend of conductivity variation with the type of alkaline salt is changed completely due to the incorporated additives. An interpretation of the LiI containing sample behavior has been explained through its influence in the gel components interactions using FT-IR spectroscopy. The highest conductivity of electrolytes with additives is exhibited by KI containing sample and it showed 3.96 mS cm^{-1} at 25 °C.

A clear trend of an open circuit voltage and efficiency enhancement with increasing cation size is observed by DSSCs in absence of performance enhancers. However, the enhancers increased the short circuit current density (J_{sc}), open circuit voltage (V_{oc}), fill factor (*ff*) and energy conversion efficiency in the entire the series of DSSCs. The performance enhancers or additives used in this work are responsible for 348, 217, 76.5, 35.8 and 22.4% efficiency enhancement for LiI, NaI, KI, RbI and CsI containing solar cells respectively. All the cells with additives have shown V_{oc} and *ff* values higher than 0.7 V and 60%, respectively. The maximum J_{sc}, and efficiency values were given by KI containing DSSCs reaching 11.35 mA cm^{-2} and 5.26%. The reported work is important to choose appropriate iodide salt to fabricate DSSCs with and without performance enhancers.

References

[1] O.A. Ileperuma, Gel polymer electrolytes for dye sensitised solar cells: a review: Material, Technol.: Advanced Performance Materials 28 (2013) 65–70.
[2] M.S. Su'ait, M.Y.A. Rahman, A. Ahmad, Review on polymer electrolyte in dye-sensitized solar cells (DSSCs), Sol. Energy 115 (2015) 452–470.
[3] J. Wu, Z. Lan, J. Lin, M. Huang, Y. Huang, L. Fan, G. Luo, Electrolytes in Dye-Sensitized Solar Cells, Chem. Rev. 115 (2015) 2136–2173.
[4] P. Baglioni, D. Chelazzi, R. Giorgi, G. Poggi, Colloid and Materials Science for the Conservation of Cultural Heritage: Cleaning, Consolidation, and Deacidification Langmuir 29 (2013) 5110–5122.
[5] T.M.W.J. Bandara, W.J.M.J.S.R. Jayasundara, H.D.N.S. Fernando, M.A.K.L. Dissanayake, L.A.A. De Silva, P.S.L. Fernando, M. Furlani, B.-E. Mellander, Efficiency enhancement of dye-sensitized solar cells with PAN: CsI: LiI quasi-solid state (gel) electrolytes, J. Appl. Electrochem. 44 (2014) 917–926.
[6] N. Han, Y. Koide, A. Chiba, R. Islam, N. Komiya, A. Fuke, Improvement of efficiency of dye-sensitized solar cells by reduction of internal resistance, Appl. Phys. Lett. 86 (2005), 213501.
[7] A. Yella, H.W. Lee, H.N. Tsao, C. Yi, A.K. Chandiran, M.K. Nazeeruddin, E.W.G. Diau, C.Y. Yeh, S.M.M. Zakeeruddin Grätzel, Porphyrin-sensitized solar cells with cobalt (II/III)-based redox electrolyte exceed 12 percent efficiency, Science 6056 (2011) 629–634.
[8] K. Kakiage, Y. Aoyama, T. Yano, K. Oya, J. Fujisawa, M. Hanaya, Highly-efficient dye-sensitized solar cells with collaborative sensitization by silyl-anchor and carboxy-anchor dyes, Chem. Commun. 51 (2015) 15894–15897.
[9] V. Gondane, P. Bhargava, Acetylacetone: a promising electrolyte solvent for dye sensitized solar cells, RSC Adv. 6 (2016) 37167–37172.
[10] L. Tao, Z. Huo, Y. Ding, Y. Li, S. Dai, L. Wang, J.X. Zhu Pan, B. Zhang, J. Yao, M.K. Nazeeruddin, High-efficiency and stable quasi-solid-state dye-sensitized solar cell based on low molecular mass organogelator electrolyte, J. Mater. Chem. A 3 (2015) 2344–2352.
[11] T.M.W.J. Bandara, H.D.N.S. Fernando, M. Furlani, I. Albinsson, M.A.K.L. Dissanayake, B.-E. Mellander, Performance enhancers for gel polymer electrolytes based on LiI and RbI for quasi-solid-state dye sensitized solar cells, RSC Adv. 6 (2016) 103683–103691.
[12] T.M.W.J. Bandara, T. Svensson, M.A.K.L. Dissanayake, M. Furlani, W.J.M.J.S.R. Jayasundara, B.-E. Mellander, Tetrahexylammonium iodide containing solid and gel polymer electrolytes for dye sensitized solar cells, Energy Procedia 14 (2012) 1607–1612.
[13] T.M.W.J. Bandara, M. Fernando, I. Albinsson, M.A.K.L. Dissanayake, J.L. Ratnasekera, B.-E. Mellander, Effect of the alkaline cation size on the conductivity in gel polymer electrolytes and their influence on photo electrochemical solar cells, Phys. Chem. Ch. Ph. 18 (2016) 10873–10881.
[14] T.M.W.J. Bandara, W.J.M.J.S.R. Jayasundara, M.A.K.L. Dissanayake, M. Furlani, I. Albinsson, B.-E. Mellander, Effect of cation size on the performance of dye sensitized nanocrystalline TiO_2 solar cells based on quasi-solid state PAN electrolytes containing quaternary ammonium iodides, Electrochim. Acta 109 (2013) 609–616.
[15] A.A. Arbab, M.H. Peerzada, I.A. Sahito, S.H. Jeong, A complete carbon counter electrode for high performance quasi solid state dye sensitized solar cell, Journal of Power Sources 343 (2017) 412–423.
[16] M.A. Andrade, K. Miettunen, A. Tiihonen, P.D. Lund, A.F. Nogueira, H.O. Pastore, Stabilizing Dendron-Modified Talc-Based Electrolyte for Quasi-Solid Dye-Sensitized Solar Cell, Electrochim. Acta 228 (2017) 413–421.
[17] M. Gerosa, A. Sacco, A. Scalia, F. Bella, A. Chiodoni, M. Quaglio, E. Tresso, S. Bianco, Toward totally flexible dye-sensitized solar cells based on titanium grids and polymeric electrolyte, IEEE Journal of Photovoltaics 6 (2) (2016) 498–505.

UNCORRECTED PROOF

[18] D.J. Zheng, M.D. Ye, X.R. Wen, N. Zhang, C.J. Lin, Electrochemical methods for the characterization and interfacial study of dye-sensitized solar cell, Sci. Bull. 60 (2015) 850–863.
[19] K. Nazeeruddin, A. Kay, I. Rodicio, R. Humphry-Baker, E. Mueller, P. Liska, N. Vlachopoulos, M. Gratzel, Conversion of Light to Electricity by cis-X_2Bis(2, 2′-bipyridyl-4, 4′-dicarboxylate)ruthenium(11) Charge-Transfer Sensitizers (X = C1-, Br-, I-, CN-, and SCN-) on Nanocrystalline TiO_2 Electrodes, J. Am. Chem. Soc. 115 (1993) 6382.
[20] S. Huang, G. Schlichthorl, A. Nozik, M. Gratzel, A. Frank, Charge Recombination in Dye-Sensitized Nanocrystalline TiO_2 Solar Cells, J. Phys. Chem. B 101 (1997) 2576.
[21] T.M.W.J. Bandara, W.J.M.J.S.R. Jayasundara, H.D.N.S. Fernando, M.A.K.L. Dissanayake, L.A.A. DeSilva, P.S.L. Fernando, M. Furlani, B.-E. Mellander, Efficiency enhancement of dye-sensitized solar cells with PAN:CsI:LiI quasi-solid state (gel) electrolytes, J. Appl. Electrochem. 44 (2014) 917–926.
[22] M. Kovač, M. Gaberšček, J. Grdadolnik, The effect of plasticizer on the microstructural and electrochemical properties of a $(PEO)_n$ $LiAl(SO_3Cl)_4$ system, Electrochim. Acta 44 (1998) 863–870.
[23] Y. Lu, Z. Tu, L.A. Archer, Stable lithium electrode position in liquid and nanoporous solid electrolytes, Nat. Mater. 13 (2014) 961–969.
[24] K. Murata, S. Izuchi, Y. Yoshihisa, An overview of the research and development of solid polymer electrolyte batteries, Electrochim. Acta 45 (2000) 1501–1508.
[25] M. Rahman, S.B. Christopher, Ionic liquids, New generation stable plasticizers for poly (vinyl chloride), Polym. Degrad. and Stabil 91 (12) (2006) 3371–3382.
[26] M. Egashira, H. Todo, N. Yoshimoto, M. Morita, Lithium ion conduction in ionic liquid-based gel polymer electrolyte, J. Power Sources 178 (2008) 729–735.
[27] B. Zhang, D.A. Hoagland, Z. Su, Ionic liquids as Plasticizers for Polyelectrolyte Complexes, J. Phys. Chem. B 119 (8) (2015) 3603–3607.
[28] S. Koneshan, J.C. Rasaiah, R.M. Lynden-Bell, S.H. Lee, Solvent structure, dynamics, and ion mobility in aqueous solutions at 25C, J. Phys. Chem. B 102 (21) (1998) 4193–4204.
[29] Q.-Y. Wu, X.-N. Chen, L.-S. Wan, Z.-K. Xu, Interactions between polyacrylonitrile and solvents: density functional theory study and two-dimensional infrared correlation analysis, J. Phys. Chem. B 116 (2012) 8321.
[30] D. Ostrovskii, A. Brodin, L. Torell, G.B. Appetecchi, B. Scrosati, Molecular and ionic interactions in poly (acrylonitrile)-and poly (methylmetacrylate)-based gel electrolytes, J Chem. Phys. 109 (1998) 7618.
[31] H. Wang, L.M. Peter, Influence of electrolyte cations on electron transport, electron transfer in dye-sensitized solar cells, J Phys. Chem. C 116 (2012) 10468–10475.
[32] M.A.K.L. Dissanayake, C.A. Thotawatthage, G.K.R. Senadeera, T.M.W.J. Bandara, W.J.M.J.S.R. Jayasundera, B.-E. Mellander, Efficiency enhancement by mixed cation effect in dye-sensitized solar cells with PAN based gel polymer electrolyte, J Photochemistry & Photobiology: A Chemistry 246 (2012) 29–35.
[33] T.M.W.J. Bandara, M.A.K.L. Dissanayake, W.J.M.J.S.R. Jayasundara, I. Albinsson, B.-E. Mellander, Efficiency enhancement in dye sensitized solar cells using gel polymer electrolytesbased on a tetrahexylammonium iodide and MgI2 binary iodide system, Phys. Chem. Ch. Ph. 4 (2012) 8620–8627.
[34] M. Gorlov, L. Kloo, Ionic liquid electrolytes for dye-sensitized solar cells, Dalton Transactions 20 (2008) 2655–2666.
[35] R. Hayes, G.G. Warr, R. Atkin, Structure and nanostructure in ionic liquidsChemical reviews 115 (13) (2015) 6357–6426.
[36] M.K. Nazeeruddin, A. Kay, I. Rodicio, R. Humphry-Baker, E. Müller, P. Liska, N. Vlachopoulos, M. Grätzel, Conversion of light to electricity by cis-X2bis(2,2'-bipyridyl-4,4'-dicarboxylate)ruthenium(II) charge-transfer sensitizers (X = Cl-, Br-, I-, CN-, and SCN-) on nanocrystalline titanium dioxide electrodes, J. Am. Chem. Soc. 115 (1993) 6382–6390.
[37] L. Dloczik, O. Ileperuma, I. Lauermann, L.M. Peter, E.A. Ponomarev, G. Redmond, N.J. Shaw, I. Uhlendorf, Dynamic response of dye-sensitized nanocrystalline solar cells: characterization by intensity-modulated photocurrent spectroscopy, J. Phys. Chem. B 101 (1997) 10281–10289.

UNCORRECTED PROOF